States in ^{22}O via β decay of ^{22}N

C. S. Sumithrarachchi,[1,2,*] D. J. Morrissey,[1,2] A. D. Davies,[1,3] D. A. Davies,[1,2]
M. Facina,[1] E. Kwan,[1,3] P. F. Mantica,[1,2] M. Portillo,[1] Y. Shimbara,[1] J. Stoker,[1,2] and R. R. Weerasiri[1,2]
[1]*National Superconducting Cyclotron Laboratory, Michigan State University, East Lansing, Michigan 48824, USA*
[2]*Department of Chemistry, Michigan State University, East Lansing, Michigan 48824, USA*
[3]*Department of Physics and Astronomy, Michigan State University, East Lansing, Michigan 48824, USA*
(Received 28 July 2009; published 8 January 2010)

The energy-level structure of ^{22}O with the recently identified $N = 14$ subshell closure was investigated by the β decay of ^{22}N for the first time. A β-delayed-neutron, time-of-flight measurement revealed six new neutron transitions attributed to the β decay of ^{22}N. One- and two-β-delayed neutron decay of ^{22}N, with emission probabilities of 33(3)% and 12(3)%, respectively, were observed to correspond to four new negative-parity states in ^{22}O. The half-life of ^{22}N β decay was determined to be 20(2) ms. Three γ-ray transitions in ^{22}O and single γ rays in ^{21}O and ^{20}O were observed following the β decay of ^{22}N. The observation of large Gamow-Teller strength for a highly excited state in ^{22}O indicates a halo structure for ^{22}N. A comparison of results with shell-model predictions showed overall poor agreement. The measured P_n values of ^{24}O and ^{25}F components of the secondary beam showed an enhancement relative to the P_n values of adjacent oxygen and fluorine isotopes, providing additional evidence for the $N = 14$ closed subshell.

DOI: 10.1103/PhysRevC.81.014302 PACS number(s): 23.40.−s, 23.20.Lv, 29.30.Hs, 27.30.+t

I. INTRODUCTION

Recent studies of exotic nuclei show a change from the general trends of nuclear structure that are found in nuclei close to the beta stability. One important change that has been identified in the region of neutron-rich light nuclei is the rearrangement of the single-particle levels, resulting in the appearance of new magic numbers as one approaches the drip line [1]. The doubly magic nature of ^{22}O is evidenced by the observation of a relatively high first excited state compared to the neighboring even-even oxygen isotopes [2]. Spectroscopic measurements of ^{20}C [3], ^{22,21}N [4,5], and ^{24}Ne [6] reveal a reduction of the shell gap at $N = 14$ toward the neutron drip line compared to ^{22}O, indicating that the subshell influence appears to be limited to oxygen and fluorine nuclei. The energy levels in these nuclei may be more complicated than those due to simply a larger subshell gap. The study of the energy levels in ^{22}O has been particularly important for understanding the rapid change in the drip line location between oxygen and fluorine [7]. The present study focuses mainly on the energy levels of ^{22}O fed by the β decay of ^{22}N using neutron and γ-ray spectroscopies.

The excitation energy of 3170(20) keV for the first 2^+ state in ^{22}O was determined via an inelastic scattering experiment by Thirolf *et al.* [2]. The γ decay in ^{22}O was later determined by Belleguic *et al.* [8] from an in-beam fragmentation experiment at the Grand Accélérateur National d'Ions Lourds (GANIL). They reported γ-ray transitions at 1310 and 3200 keV and confirmed the assignment of the 3200-keV γ ray as the $2^+_1 \rightarrow 0^+_{gs}$ transition in ^{22}O, and the other attributed to the decay of a higher excited state to the 2^+_1 state. The energy level scheme for ^{22}O with positive-parity states has been recently extended by Stanoiu *et al.* using single and two-step fragmentation experiments at GANIL [9]. They reported five excited states in ^{22}O derived from γ rays at 1383(4), 1710(90), 2354(6), 3199(8), 3310(90), and 3710(90) keV. The spins and parities of the states were based on shell-model calculations. A knockout experiment carried out at GSI to measure the longitudinal momentum distribution for neutron-rich oxygen isotopes reported a γ spectrum with the three γ-ray energies of 1.3, 2.6, and 3.2 MeV from the deexcitation of ^{22}O [10]. The first two γ-ray transitions were assigned to a negative-parity state (0^- or 1^-) at 5.8 MeV, which deexcited into the 2^+ and 3^+ states at 3.2 and 4.5 MeV, respectively. This negative-parity assignment was deduced based on arguments by Brown *et al.*, who calculated the spectroscopic factors in the ^{12}C(^{23}O,^{22}O)X reaction [11]. The ground state and the first excited state of ^{22}O have also been studied using an ^{22}O(p, p') reaction, reconfirming the $N = 14$ subshell closure in ^{22}O by probing the proton and neutron contributions to the 2^+ excitation [12]. The negative-parity states in ^{22}O are not experimentally known except for the proposed state at 5.8 MeV. However, the β decay of the presumed negative-parity ground state of the odd-mass nitrogen isotopes can provide information on the negative-parity states in the even-even oxygen isotope daughters.

Mueller *et al.* [13] reported the β-decay half-life of ^{22}N to be $24(+7-6)$ ms while Reeder *et al.* [14] found a shorter half-life of 14(6) ms. The total neutron emission probability P_n was deduced to be 35(5)% for the ^{22}N β decay [13]. More recent work done by Yoneda *et al.* [15] reported the β-delayed neutron multiplicities for ^{22}N to be $P_{1n} = 41(+12-10)$% and $P_{2n} < 13$% with a half-life of $16.5(+8.5-4.8)$ ms. Although the half-lives and P_n values agree to within the errors, the uncertainties are large. There is no spectroscopic information

*Present address: Department of Physics, University of Guelph, Guelph, Ontario N1G 2W1, Canada; chandana@physics.uoguelph.ca

reported on the β decay of ^{22}N. The first excited state at 183 keV and the second excited state at 1012 keV in ^{22}N have recently been measured [4]. The spins and parities of 1^- and 2^-, respectively, for the states just discussed and of 0^- for the ground state were given based on the comparison with the shell-model calculation. In addition, ^{22}N was predicted to be a one-neutron halo nucleus using the neutron cluster-core model by Gupta *et al.* [16]. The β decay of halo nuclei have a large fraction of the β-decay strength going to high-energy states [17]. Thus, the present measurement of β-decay branching ratios can provide important new information on the structure of ^{22}N.

II. EXPERIMENTAL DETAILS

A ^{22}N secondary beam was produced by fragmentation of a 140 MeV/A ^{48}Ca primary beam, delivered by the coupled cyclotron facility of the National Superconducting Cyclotron Laboratory (NSCL), in an 846-mg/cm^2 Be target. The A1900 fragment separator, along with an 825-mg/cm^2 Al wedge, was used in an energy-loss mode to produce the ^{22}N beam. The secondary beam was a cocktail whose major constituents were ^{22}N, ^{25}F, and ^{24}O. The desired fragment was fully stopped in a thin plastic implantation detector after passing through a 15.704-mm thick Al degrader. The purity of the implanted nuclei was analyzed with silicon detectors located before and after the implantation detector. The composition of the implanted beam and their known half-lives are given in Table I. The beam was pulsed with a beam on/off time of 100 ms in order to collect nuclei and monitor the β decay. The detailed experimental setup and the calibration procedures used in this experiment can be found in Refs. [18,19].

The β-delayed neutrons were measured using a neutron spectroscopic array with sixteen neutron detectors [20], which had a total neutron detection efficiency of 2.26% at 1.0 MeV. The implantation detector was placed at the center of the neutron array in order to have an equal flight path of approximately 1 m for all neutrons. β-delayed neutrons from ^{16}C and ^{17}N were used to establish energy, efficiency and peak shape calibrations for the neutron array. Eight detectors from the NSCL Segmented Germanium Array (SeGA) [21] with a total β-γ coincidence efficiency of 1.9% at 1.0 MeV were used to measure coincident β-delayed γ rays.

TABLE I. Composition of the implanted beam and published half-lives.

Nuclide	Purity at implantation detector (%)	Half-life (ms)
^{22}N	51.8	24(5)[a]
^{25}F	35.6	90(9)[b]
^{24}O	12.6	65(5)[c]

[a]Average from Refs. [13,15,22].
[b]From Ref. [23].
[c]From Ref. [24].

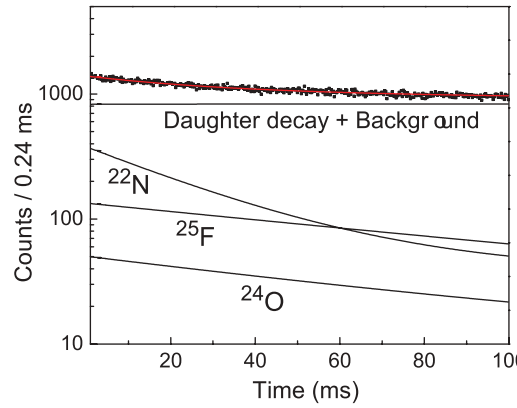

FIG. 1. (Color online) Total β-decay curve obtained from the implanted beam. The graph shows the total decay curve, the individual decay components of ^{22}N, ^{25}F, and ^{24}O, and the background plus all decay contributions of daughter and granddaughter decay.

III. RESULTS

A. The total β-decay curve

The total β-decay curve for the ^{22}N cocktail beam recorded during the beam-off period of 100 ms is shown in Fig. 1. Although this decay curve has contributions from the β decays of the ^{22}N, ^{25}F, and ^{24}O decay series, the total number of β-decay events from the individual decays can be extracted by fitting the data with an appropriate decay model. The model was developed using the Bateman equations for all implanted decay series and incorporated the beam on/off conditions.

The fit to the decay data was performed, where the half-life, the total neutron emission probability, the initial activity of ^{22}N, and a flat background were variables. The half-lives of ^{25}F and ^{24}O, which were found from the γ-ray-gated decay curves to be 73(11) and 53(8) ms, respectively, and the half-lives of all daughters and granddaughters in the series, taken from the literature, were included in the model as fixed values. In addition, the reported neutron emission probabilities of 23(5)% and 58(12)% for ^{25}F and ^{24}O, respectively, were included in the model [23,24]. The fraction of the initial activities of each implanted decay series was fixed based on the composition of the implanted beam. The individual decay contributions from the fitting process and the total fit to data are shown in Fig. 1. The total number of β-decay events taken by integrating the individual curves for the implanted nuclei are given in Table II with half-lives determined in this work.

TABLE II. The detected β-decay events from the implanted nuclei.

Nuclide	Total number of β-decay events	Half-life (ms)
^{22}N	$5.58(2) \times 10^4$	21(7)[a]
^{25}F	$3.84(4) \times 10^4$	73(11)[b]
^{24}O	$1.37(4) \times 10^3$	53(8)[b]

[a]By fitting the decay data.
[b]From γ-ray-gated half-lives.

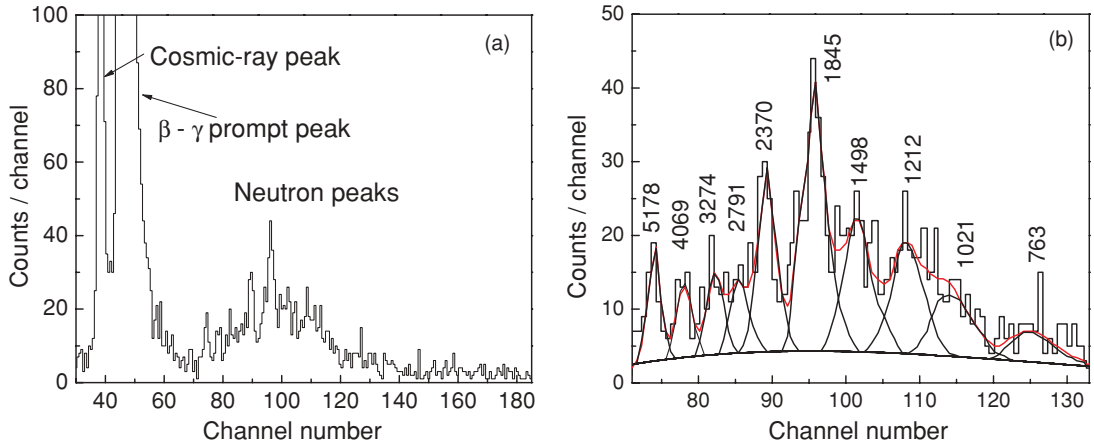

FIG. 2. (Color online) β-delayed-neutron, time-of-flight spectrum from the decay of implanted nuclei. Panel (a) shows the β-γ prompt peak, and the peak due to cosmic-ray interactions with the neutron detectors are shown in addition to the neutron peaks. Panel (b) shows the fitted neutron peaks and the background. The neutron peak energies are given in keV above each peak.

B. β-delayed neutron analysis

The β-delayed-neutron time-of-flight spectrum, shown in Fig. 2, was produced by adding all neutron detector data after individual correction for any time walk in each constant-fraction discriminator. The β-γ prompt peak was used as a time reference for the neutron energy measurements. The peak labeled as the cosmic-ray peak in Fig 2(a) was produced by cosmic rays passing first through the neutron detectors and then triggering the implantation detector. The peaks to the right of the β-γ prompt peak in Fig. 2(a) are neutron peaks originating from β decay of the implanted nuclei.

The expanded neutron peaks region is shown in Fig. 2(b). The peak shapes, which are energy dependent, were established by a shape calibration using the known neutrons from ^{16}C and ^{17}N β decay. The neutron peaks were fit with ten asymmetric Gaussians, given the constraints of the shape calibration and a variable background, which were also studied with the β-delayed-neutron, time-of-flight spectra of ^{16}C and ^{17,19,20}N for the same geometry. Figure 2(b) shows the fitted neutron peaks labeled by neutron energies in keV and a third-order polynomial background.

The possibility of different numbers of peaks in the spectrum, especially in the flat regions of the spectrum, was explored. A reasonable fit was not found with a greater or lesser number of peaks under the peak shape constraints. Narrow gates were applied around the neutron peaks to generate gated decay curves, which were used to assign each neutron peak. The decay curves, shown in Fig. 3, were fit with a single decay component and a flat background. The neutron-gated decay curves generated from the neutron peaks of 2791, 3274, and 4069 keV, which are closely overlapped, are not shown due to their poor statistics. The gated half-lives of neutron energies at 763, 1021, 1498, 1845, 2370, and 5178 keV are consistent with the β decay of ^{22}N. The neutron energy at 1212 keV was identified as a contaminant based on the longer half-life of 68(16) ms relative to the half-life of ^{22}N.

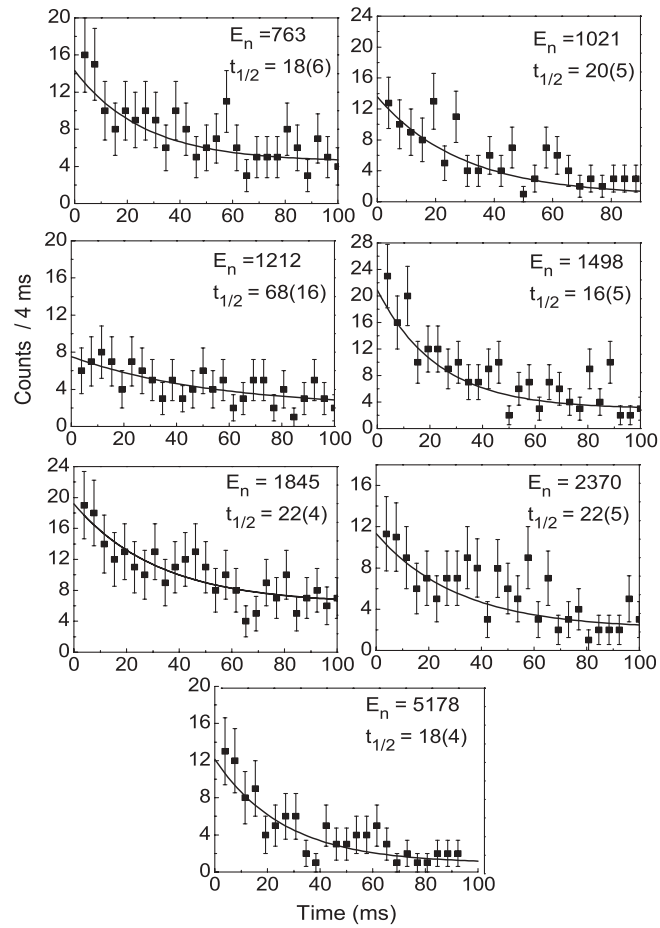

FIG. 3. Neutron-gated decay curves. The neutron energies (keV) and the gated half-lives (ms) are shown.

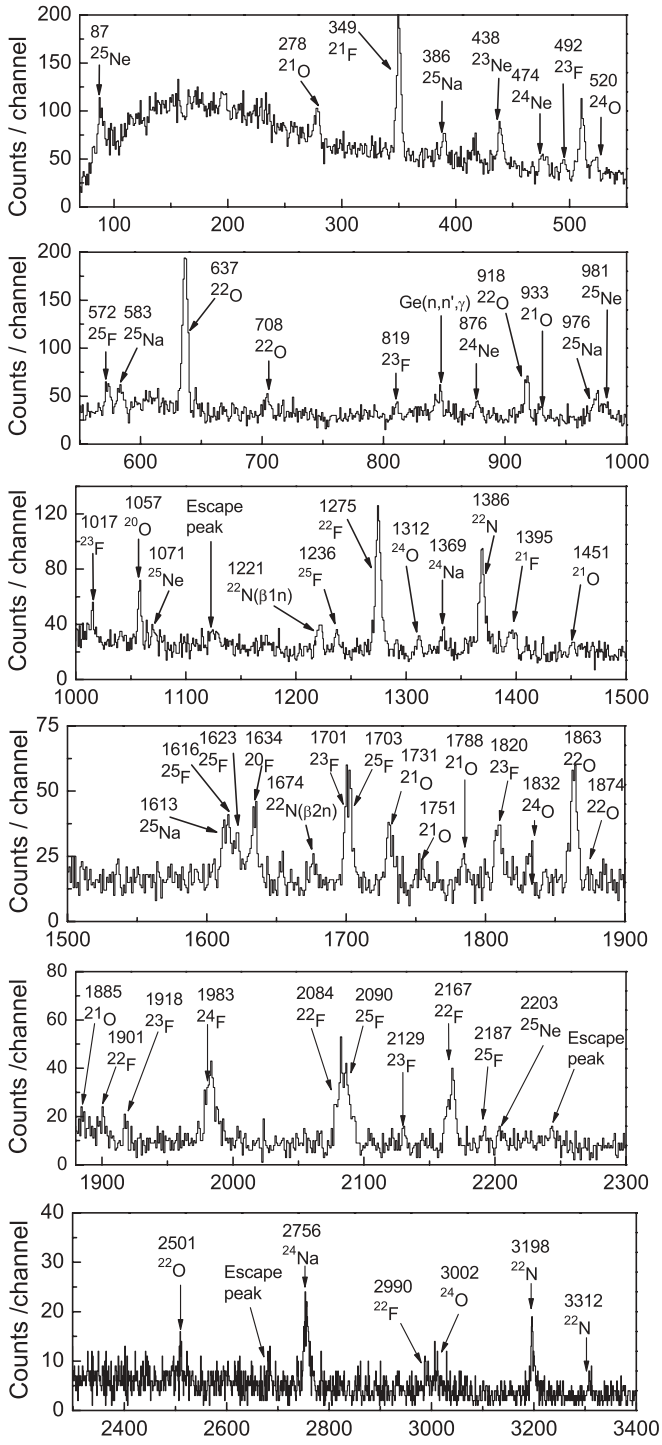

FIG. 4. Total β-γ coincidence spectrum from the implanted cocktail beam. The peaks are labeled by their parent nuclide and γ-ray energy.

C. β-delayed γ-ray analysis

The total β-γ coincidence spectrum obtained for the ^{22}N cocktail beam, shown in Fig. 4, contains the β-delayed γ-ray events from the ^{22}N, ^{25}F, and ^{24}O β-decay chains accumulated during the beam-off time period. The identified γ-ray transitions are labeled by the parent nucleus. The transitions with energies of 637, 708, 918, 1863, 1874, and 2501 keV are consistent with the γ-ray transitions reported by Hubert *et al.* [25] and by Weissman *et al.* [26] in the β decay of ^{22}O, the daughter of the ^{22}N β decay. The observed relative intensities of these γ rays also confirm the assignments. The γ-ray peak at 72 keV, which was observed in the ^{22}O β decay [26], was not clearly visible in the spectrum due to the thresholds of the SeGA detectors. The γ-ray transitions at 1275, 1901, 2084, 2167, 2990, and 4368 keV in the β decay of ^{22}F (the granddaughter of ^{22}N) reported by Davids *et al.* [27] were also observed in the present work.

The remaining γ-ray transitions associated with the β decay of ^{22}F reported by Davids *et al.* were not visible in the current work because of the poor statistics. The γ-ray transitions at 278, 933, 1451, 1731, 1751, 1788, and 1885 keV attributed to the β decay of ^{21}O (the β-delayed neutron daughter of ^{22}N) published by Alburger *et al.* [28] were observed in this work. The rest of the γ rays reported in Ref. [28] were not intense enough to be observed in the spectrum. The γ rays at 349 and 1395 keV, shown in Fig. 4, were attributed to ^{21}F β decay, which is the granddaughter in the decay chain for $A = 21$ [29,30].

Apart from the γ rays associated with the direct β-decay chain and the β-delayed one-neutron daughter decay chain of ^{22}N, γ rays from the $A = 20$ mass chain, which were not implanted in this experiment, were found in the β-γ coincidence spectrum. The γ-ray transitions at 1057 and 1634 keV were assigned to ^{20}O and ^{20}F, respectively, based on their gated half-lives and known states. The only mechanism that can explain the production of the $A = 20$ mass chain is the sequential emission of two neutrons following the β decay of ^{22}N. In addition, the known 1674-keV γ ray in ^{20}O was observed as reported in Ref. [18], whereas the other γ rays in ^{20}O were not observed. This fact justifies that the $A = 20$ decay chain originated from the β decay of ^{22}N. The 1386, 3198, and 3312-keV γ-ray transitions, shown in Fig. 4, were identified as transitions in ^{22}O [9]. The rest of transitions in ^{22}O reported in Refs. [9,10] were not observed. The γ ray at 1221 keV, which was reported in the work of Stanoiu *et al.* [9], was identified as arising from a γ-ray transition in ^{21}O. The other γ rays reported in the same work were not seen. Although the observed 2129(4)-keV γ ray was consistent with the reported γ ray at 2133(5) keV in ^{21}O within uncertainties, it was assigned to the β decay of ^{23}F based on the relative intensities.

The 1221- and 3198-keV γ-ray-gated decay curves, shown in Fig. 5, were fit with a single exponential function and a flat background to extract the gated half-lives. The deduced half-lives and their respective gated energies are shown in the figure. The agreement between the observed half-lives and the published half-life for ^{22}N confirmed the assignments. The gated decay curves for γ rays at 1674 and 3312 keV were too weak to extract accurate half-lives.

D. β-decay scheme of ^{22}N

The summary of γ-ray and neutron assignments is given in Table III and the proposed β-decay scheme of ^{22}N is shown in Fig. 6. The gated decay curve analysis of the neutron time-of-flight spectrum showed six neutron peaks that originated from

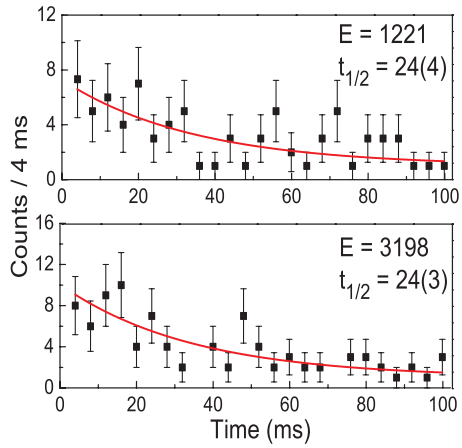

FIG. 5. (Color online) γ-ray-gated decay curves. The gated γ-ray peak energies (keV) and corresponding half-lives (ms) are given.

TABLE III. Assignments of γ-ray and neutron energies for β decay of ^{22}N.

γ-ray energy (keV)	Emission probability (%)	Half-life (ms)	Nuclide	Energy level (keV)
1386(4)	7(3)	–	^{22}O	4584
3198(8)	24(3)	24(3)	^{22}O	3198
3312(5)	2.0(10)	–	^{22}O	6510
1221(3)	7.0(11)	24(4)	^{21}O	1221
1674(3)	2.2(12)	–	^{20}O	1674
Neutron energy (keV)	Emission probability (%)	Half-life (ms)	Nuclide	Energy level (keV)
763(1)	12(3)	18(6)	^{22}O	7649
1845(4)	13(1)	22(4)	^{22}O	8783
2370(6)	6.6(7)	22(5)	^{22}O	10554
1021(2)[a]	9.6(16)	20(5)	^{22}O	13298
1498(3)[a]	9.2(10)	16(5)	^{21}O	5379[b]
5178(24)	3.1(6)	18(4)	–	–

[a]Assignment could be interchanged.
[b]This could be moved to the level at 4878 keV.

the β decay of ^{22}N. The γ ray at 1221 keV was assigned to the level at 1221 keV in ^{21}O, consistent with previous work [9]. This γ-ray transition required a feeding of 7.0%, which could be satisfied by the neutron transition of energy 2370 keV. Therefore, the 2370-keV neutron transition was assigned to the state at 10545 keV in ^{22}O.

The analysis of the γ-ray activities of ^{21}O provided the one-neutron emission probability of 33(3)%. This suggested a feeding requirement of 26(3)% to the ground state of ^{21}O. (Note that the parent and daughter activities in this decay series were saturated during the 30-minute-long runs; thus, it was reasonable to estimate emission probabilities from the daughter activity.) The neutron energies at 763 and 1845 keV were placed at 7649 and 8783 keV in ^{22}O, respectively, as shown in Fig. 6, in order to feed the ground state of ^{21}O because they cannot fulfill any other intensity requirement for states in the ^{22}N β decay. The observation of a γ ray at 1674 keV in ^{20}O suggested the presence of β-delayed-neutron decays to neutron unbound states in ^{21}O, which subsequently decay to the neutron bound states in ^{20}O. The energy levels in ^{20}O are well-known from previous experiments [9,18] and the 1674-keV γ ray was observed depopulating the 1674-keV state in ^{20}O. The difference of 9.8(4)% between the γ-ray feeding to the ground state of ^{20}O and the number of ^{20}O β-decay events derived from the daughter γ-ray activities suggested some neutron feeding to the ground state of ^{20}O. Two neutrons with energies of 1021 and 1498 keV emitted in sequence match with the feeding requirement to the ground state of ^{20}O because they have the same neutron emission probabilities [9.6(16)% and 9.2(10)%, respectively].

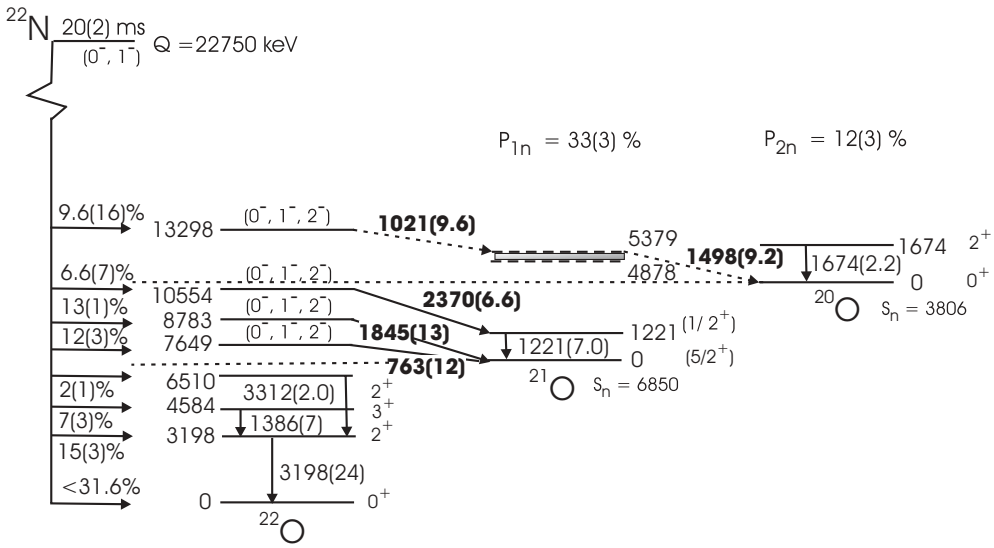

FIG. 6. β-decay scheme of ^{22}N. The energy levels in ^{20,21,22}O are shown with their energies (keV), spins, and parities. Neutron and γ-ray transition energies (keV) are given near to transitions with their emission probabilities in parentheses. The values on horizontal arrows represent the β-decay feedings with their uncertainties.

The β-delayed neutron-neutron coincidence events were not observed due to a low neutron detection efficiency. However, there were two possible ways to order these neutron transitions. One way is to assign the 1021 keV neutron as depopulating a 13298-keV state in ^{22}O and to connect the 1498-keV neutron to a state at 5379 keV in ^{21}O. The second way is to interchange the order of emission. The proposed 5379-keV state in ^{21}O would then be lowered by 501 keV, whereas the proposed level in ^{22}O would remain unchanged. The uncertainty of this intermediate level in ^{21}O is represented by a shaded box in Fig. 6. The feeding to the state at 1674 keV in ^{20}O was possible with the sequential emission of the 5178-keV neutron and one of the neutrons with 2791, 3274, or 4069 keV, since they have similar emission probabilities, or low energy neutrons that are below the detection limit of the neutron array. However, these neutrons were not assigned to states as they are associated with low emission probabilities. The γ-ray transitions at 1386, 3198, and 3312 keV were placed in the ^{22}O levels, as given in Table III, to be consistent with previous work [9]. The β-delayed γ-γ coincidence events were not observed due to poor statistics.

Figure 6 shows decay to the one-neutron daughter ^{21}O with a one-neutron emission probability of 33(3)% and to the two-neutron daughter ^{20}O with a two-neutron emission probability of 12(3)%. The total neutron emission probability for the β decay of ^{22}N was deduced to be 57(5)%, which is in reasonable agreement with recent literature values [15,22]. An adopted half-life of 20(2) ms for the ^{22}N β decay, shown in Fig. 6, was deduced from the neutron- and γ-ray-gated decay curves shown herein and the half-life value given in Table II and derived from the fit to the total β-decay curve. The β branches for excited states in ^{22}O, shown in Fig. 6, have been calculated by considering the intensity flow through the decay scheme. The upper limit of β-decay feeding to the ground state was calculated from the β-decay activity of ^{22}O. The transition probabilities for both neutrons and γ rays are given in parentheses following the transition energy. The neutron decay of the highest observed energy level in ^{22}O is displayed with a dashed line because of the large uncertainty in the assignment. The apparent log *ft* values reported in Table IV were calculated as explained in Ref. [31] using a Q-value of 22750 keV [32], a half-life of 20 ms, and the observed β-decay branching ratios.

TABLE IV. Properties of the ^{22}N β decay.

Energy level (keV)	Branch (%)	Log *ft*	Spin parity	B(GT)
0	<31.6	5.82	0^+	–
3198	15(3)	5.79	2^+	–
4584	7(3)	5.95	3^+	–
6510	2(1)	6.24	2^+	–
7649	12(3)	5.30	$0^-, 1^-, 2^-$	0.020
8783	13(1)	5.09	$0^-, 1^-, 2^-$	0.032
10554	6.6(7)	5.08	$0^-, 1^-, 2^-$	0.033
13298	9.6(16)	4.36	$0^-, 1^-, 2^-$	0.17

Four states in ^{22}O were assigned as negative-parity states whereas the observed neutron bound states were kept as positive-parity based on the log *ft* values and the β-decay selection rules. Since the energy gap between the 0^- ground state and the 1^- first excited state in ^{22}N was measured to

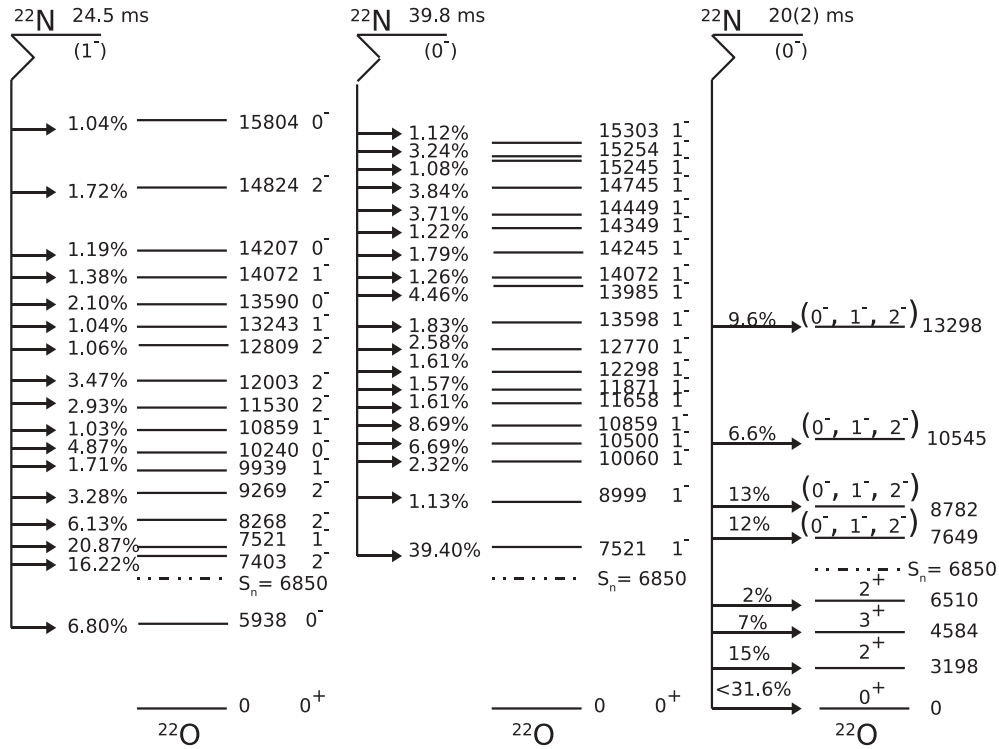

FIG. 7. Theoretically allowed β-decay schemes of ^{22}N (left and center) compared to the present experiment. The feeding of levels in ^{22}O calculated based on the shell model for different ground-state spins with β-decay branches higher than 1% are shown.

be small, we assume the spin and parity of the ground state of ^{22}N could be 0^- or 1^-. Thus, the possible spins for the negative-parity states are 0, 1, or 2 based on the allowed β decay of the ^{22}N ground state. All bound states observed in the present work were known in previous experiments. The spins of the positive-parity bound states in ^{22}O should be 0, 1, 2, or 3 to satisfy the selection rules of the first forbidden decay. However, the spins of the bound states, shown in Fig. 6 and Table IV, were taken mostly from previous work. The spins and parities for states in ^{21}O and ^{20}O were taken from Refs. [9,18]. The Gamow-Teller strengths B(GT) for β decay to the assigned negative-parity states in ^{22}O were calculated as explained in Ref. [33] and are given in Table IV for comparison with shell-model calculations.

IV. DISCUSSION

A. Shell-model calculations for ^{22}N

Shell-model calculations have been performed for the allowed β decay of ^{22}N using the WBP interaction in the *spsdpf* shell-model space to compare with the experimental results. The calculations were performed assuming the ground state of ^{22}N is either 0^- or 1^- and only take into account the allowed Gamow-Teller transitions to negative-parity final states. The β-decay half-lives of ^{22}N were calculated to be 39.8 and 24.5 ms for the 0^- or 1^- ground-state spin and parity assignments, respectively, and agree with the experimental half-life to within a factor of two.

In Fig. 7, we show the calculated allowed β-decay schemes of ^{22}N for the 0^- and the 1^- ground-state spin and parity assignments, compared with the observed β-decay scheme of ^{22}N in the present work. Note that the theoretical decay schemes show only the allowed β-decay branches that are larger than 1%. The calculations with the 1^- ground state show a 6.80% allowed β-decay feeding of one state below the neutron separation energy, and the rest goes to neutron unbound states. The calculations with a 0^- ground state predict that all of the allowed β decay feeds neutron unbound states. Note that the locations of the calculated energy levels in ^{22}O could change dramatically as the estimated uncertainty of the energies is about 1 MeV. In comparison, all allowed beta decay observed in the present experiment, which is 41% of the total beta decay, feeds neutron unbound states in ^{22}O. However, the overall allowed β-decay feeding pattern is not matched with either calculation.

The experimental B(GT) values for the allowed β decay of ^{22}N are also compared with those calculated with either a 0^- or a 1^- ground state for ^{22}N in Figs. 8(a), 8(b), and 8(c). Note that only the predicted B(GT) values that are higher than 0.01 and that are produced with a β branch greater than 0.5% are shown in Figs. 8(b) and 8(c). The values from both calculations are only in reasonable agreement with the experimental values in the energy range of 7–11 MeV. The single state at 13.3 MeV with the highest B(GT) value may be related to the calculated states in the energy regime around 14–16 MeV. The lower limit for the B(GT) value associated with the neutron unbound state in ^{22}O that decays by sequential neutron emission to the 1674-keV level in ^{20}O was estimated to be 0.85

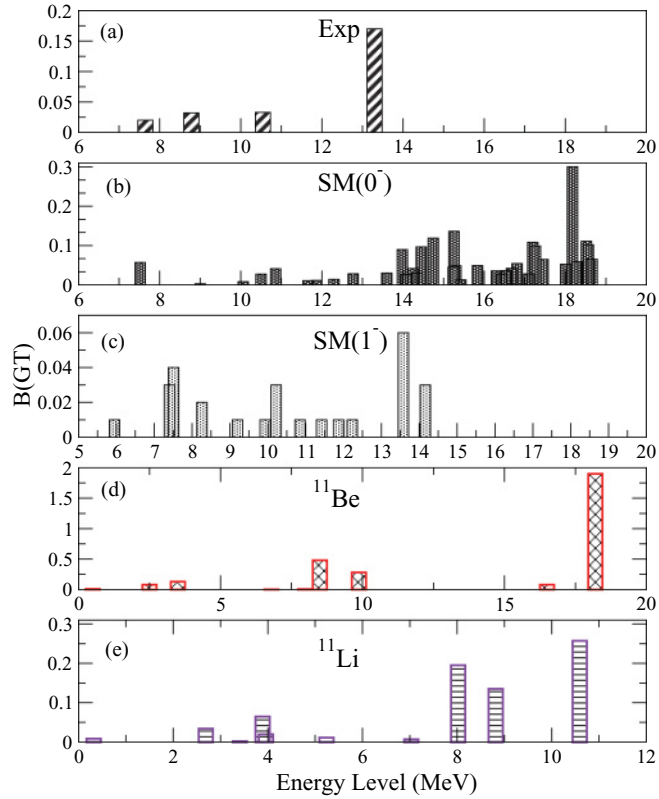

FIG. 8. (Color online) Comparison of experimental B(GT) values (a) with the shell-model predictions performed with the two possible ground-state spins of ^{22}N (b) and (c) along with the B(GT) distributions from the β decay of the halo nuclei ^{11}Be (d) and ^{11}Li (e) [34,36–38].

[$\log ft = 3.67$] assuming a β branch of 2.2% with the lower energy limit of 17767 keV for the level. This could correspond to the shell-model predicted state at 18.2 MeV with high B(GT) value.

The observation of the large B(GT) strength at high energy in ^{22}O could indicate that the large spatial extension of the ground state of ^{22}N [17] is not matched well with the low-energy structure of ^{22}O. A similar feature has been observed in the β decay of the two well-known halo nuclei ^{11}Be and ^{11}Li. The relationship between B(GT) values and the halo structure has long been suggested as a probing technique for halo structures [34,35]. For example, the B(GT) value of 1.9 associated with the ^{11}Li β transition into a high-lying state at 18.2 MeV in ^{11}Be implies a significant spatial overlap of this state and the ground state of ^{11}Li. The B(GT) values for ^{11}Be and ^{11}Li are shown in Figs. 8(d) and 8(e), where the transitions carrying the largest strength populate highly excited states [34,36–38]. The large B(GT) for the β decay of ^{22}N supports a halo structure for the ^{22}N ground state, which was predicted from the neutron cluster-core model by Gupta *et al.* [16].

B. Half-lives and neutron emission probabilities of neutron-rich light nuclei

The half-lives and neutron emission probabilities of implanted ^{25}F and ^{24}O were also measured in the present

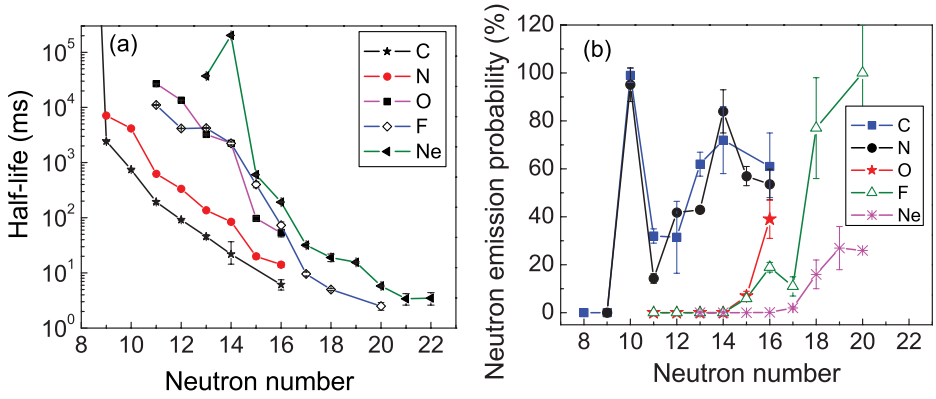

FIG. 9. (Color online) Half-life (a) and neutron emission probabilities (b) as a function of the neutron number for elements with $6 \leqslant Z \leqslant 10$.

experiment in addition to the values for ^{22}N. The variation of the experimental half-lives with increasing neutron number in neutron-rich light nuclei is shown in Fig. 9(a). The half-lives were taken from the present work and from the Nuclear Data Base [32]. The general trend of decreasing half-life with increasing neutron number (because of the decreasing binding energy) is apparent. The discontinuity at $N = 14$ for oxygen and neon isotopes is also clear and serves as another indicator of a neutron subshell closure in these isotopes.

Presented in Fig. 9(b) are the total neutron emission probabilities taken from Refs. [32,39] and from the present work for ^{22}N, ^{25}F, and ^{24}O. A discontinuity at $N = 10$ for carbon and nitrogen is noted and attributed to the influence of the $N = 8$ closed shell. The peak in P_n at $N = 14$ for nitrogen isotopes (^{21}N) cannot be explained based on the argument that the $N = 14$ closed subshell has extra stability because the neutron daughter of ^{21}N does not belong to a closed-shell configuration. The increase at $N = 16$ for oxygen and fluorine isotopes indicate the extra stability due to $N = 14$ subshell closure. The isotopes ^{24}O and ^{25}F located at the tip of the peak have β-delayed neutron daughters of ^{23}F and ^{24}Ne, respectively, that have extra stability due to $N = 14$ shell closure and, thus, more feeding to high-lying states in the daughter that lead to neutron emission probabilities. A similar argument is not true for neon isotopes because no peak is visible at $N = 16$. The overall analysis shows the influence of shell closure at $N = 14$ on the β-decay properties, particularly with oxygen and fluorine isotopes.

V. SUMMARY

The feeding of the energy levels in ^{22}O were obtained from the β decay of ^{22}N for the first time. Neutron time-of-flight and γ-ray spectroscopic measurements in coincidence with β decay showed feeding of four new negative-parity states and three positive-parity states in ^{22}O. All negative-parity states fed by the allowed β decay are neutron unbound states in ^{22}O. The large B(GT) to highly excited states in ^{22}O is indicative of a halo structure for the ^{22}N ground state. Single- and two-neutron emission probabilities were found to be 33(3)% and 12(3)%, respectively, and an adopted half-life was determined to be 20(2) ms for ^{22}N.

ACKNOWLEDGMENTS

The authors greatfully acknowledge B. A. Brown for his shell-model calculations and fruitful discussions. We would like to thank the staff of the NSCL for their assistance during the experiment. This work was supported by the National Science Foundation under Grants PHY-01-10253 and PHY-06-06007.

[1] I. Tanihata, Nucl. Phys. **A682**, 114c (2001).
[2] P. G. Thirolf, B. V. Pritychenko, B. A. Brown, P. D. Cottle, M. Chromik, T. Glasmacher, G. Hackman, R. W. Ibbotson, K. W. Kemper, and T. Otsuka, Phys. Lett. **B485**, 16 (2000).
[3] M. Stanoiu *et al.*, Phys. Rev. C **78**, 034315 (2008).
[4] D. Sohler *et al.*, Phys. Rev. C **77**, 044303 (2008).
[5] M. J. Strongman *et al.*, Phys. Rev. C **80**, 021302 (2009).
[6] C. R. Hoffman *et al.*, Phys. Rev. C **68**, 034304 (2003).
[7] H. Sakurai *et al.*, Phys. Lett. **B448**, 180 (1999).
[8] M. Belleguic *et al.*, Nucl. Phys. **A682**, 136c (2001).
[9] M. Stanoiu *et al.*, Phys. Rev. C **69**, 034312 (2004).
[10] D. Cortina-Gil *et al.*, Phys. Rev. Lett. **93**, 062501 (2004).
[11] B. A. Brown, P. G. Hansen, and J. A. Tostevin, Phys. Rev. Lett. **90**, 159201 (2003).
[12] E. Becheva *et al.*, Phys. Rev. Lett. **96**, 012501 (2006).
[13] A. C. Mueller *et al.*, Nucl. Phys. **A513**, 1 (1990).
[14] P. L. Reeder, R. A. Warner, W. K. Hensley, D. J. Vieira, and J. M. Wouters, Phys. Rev. C **44**, 1435 (1991).
[15] K. Yoneda *et al.*, Phys. Rev. C **67**, 014316 (2003).
[16] R. K. Gupta, M. Balasubramaniam, R. K. Puri, and W. Scheid, J. Phys. G **26**, L23 (2000).
[17] T. Nilsson, G. Nyman, and K. Riisager, Hyperfine Interact. **129**, 67 (2000).
[18] C. S. Sumithrarachchi, D. W. Anthony, P. A. Lofy, and D. J. Morrissey, Phys. Rev. C **74**, 024322 (2006).
[19] C. S. Sumithrarachchi *et al.*, Phys. Rev. C **75**, 024305 (2007).
[20] R. Harkewicz, D. J. Morrissey, B. A. Brown, J. A. Nolen, N. A. Orr, B. M. Sherrill, J. S. Winfield, and J. A. Winger, Phys. Rev. C **44**, 2365 (1991).

[21] W. F. Mueller, J. A. Church, T. Glasmacher, D. Gutknecht, G. Hackman, P. G. Hansen, Z. Hu, K. L. Miller, and P. Quirln, Nucl. Instrum. Methods A **466**, 492 (2001).
[22] Y. E. Penionzhkevich, Phys. At. Nucl. **64**, 1121 (2001).
[23] S. W. Padgett *et al.*, Phys. Rev. C **72**, 064330 (2005).
[24] A. T. Reed *et al.*, Phys. Rev. C **60**, 024311 (1999).
[25] F. Hubert, J. P. Dufour, R. Del Moral, A. Fleury, D. Jean, M. S. Pravikoff, H. Delagrange, H. Geissel, K.-H. Schmidt, and E. Hanelt, Z. Phys. A **333**, 237 (1989).
[26] A. L. L. Weissman *et al.*, J. Phys. G **31**, 553 (2005).
[27] C. N. Davids, D. R. Goosman, D. E. Alburger, A. Gallmann, G. Guillaume, D. H. Wilkinson, and W. A. Lanford, Phys. Rev. C **9**, 216 (1974).
[28] D. E. Alburger, C. J. Lister, J. W. Olness, and D. J. Millener, Phys. Rev. C **23**, 2217 (1981).
[29] W. R. Harris and D. E. Alburger, Phys. Rev. C **1**, 180 (1970).
[30] E. K. Warburton and D. E. Alburger, Phys. Rev. C **23**, 1234 (1981).
[31] N. B. Gove and M. J. Martin, Nucl. Data Tables **10**, 205 (1971).
[32] http://www.nndc.bnl.gov/ensdf/.
[33] K. W. Scheller *et al.*, Nucl. Phys. **A582**, 109 (1995).
[34] M. Madurga *et al.*, Phys. Lett. **B677**, 255 (2009).
[35] M. J. G. Borge *et al.*, Nucl. Phys. **A613**, 199 (1997).
[36] F. Ajzenberg-Selove, Nucl. Phys. **A506**, 1 (1990).
[37] F. Sarazin *et al.*, Phys. Rev. C **70**, 031302(R) (2004).
[38] Y. Hirayama, T. Shimoda, H. Izumi, A. Hatakeyama, K. P. Jackson, C. D. P. Levy, H. Miyatake, M. Yagi, and H. Yano, Phys. Lett. **B611**, 239 (2005).
[39] J.-L. Lou *et al.*, Chin. Phys. Lett. **25**, 1992 (2008).